מכון ויצמן למדע
WEIZMANN INSTITUTE OF SCIENCE

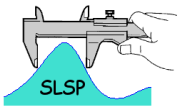

IAEA
International Atomic Energy Agency

Spectral Line Shapes in Plasmas
Code Comparison Workshop

April 2–5, 2012

Vienna, Austria

Call for Submissions

Introduction

This document is intended to define the particulars of the workshop submissions. In the sections below we define the case problems, the comparison quantities which we require and the detailed format of the data files that we will be expecting.

The webpage of the meeting is at http://plasma-gate.weizmann.ac.il/slsp/. The submission files are to be uploaded to the same server using a web interface with userid and password. Details will be announced separately.

Timeline:

February 1	—	web interface for file uploads opens
March 9	—	hotel booking deadline
March 15	—	case submission deadline
April 2	—	workshop opens
April 5	—	workshop adjourns

Contents

1 Statement of cases

We have selected a number of transitions to consider, given in Table 1. For each transition we are requesting results on a grid of electron densities (n_e) and temperatures ($T = T_\mathrm{e} = T_\mathrm{i}$). For each case, the atomic and plasma models are specified, and for some cases, there are more than one atomic or plasma model suggested. (Unless specified otherwise, plasma is assumed quasi-neutral, consisting of electrons and a single type of ions. For example, the plasma model in Case 3 is described as "Plasma ions: protons", meaning the plasma consists of electrons and protons of an equal density.) In addition, some cases are further detailed by specifying extra parameters, such as the magnetic field. Therefore, subcases for each case are defined on a four-dimensional grid.

Each calculation will be referenced by its subcase name. The subcase name is of the form Case_ID.N.T.M.F, where Case_ID is from the first column of Table 1, and the N, T, M, and F correspond, respectively, to the n_e, T, model, and external-field indices, each counting from 1. For example, 1.2.3.1.1 identifies H Lyman-α, calculated for $n_e = 10^{18}\,\mathrm{cm}^{-3}$ and $T = 100\,\mathrm{eV}$, assuming only electrons as perturbers. Similarly, 11.2.1.1.3 stands for D Balmer-β in a deuterium plasma with $n_e = 10^{15}\,\mathrm{cm}^{-3}$ and $T = 1\,\mathrm{eV}$, and magnetic field 10 T.

The models suggested are limited – some by design, others by necessity, to make them manageable without too much computational resources and human time spent. If you feel that the best suggested model for a particular case is still too far from reality, you are encouraged to submit a separate result using an alternative model you see fit best, using "0" as the model index. E.g., 3.2.1.0.1 would designate the H $n = 6 \to 5$ transition calculated for $n_e = 2 \times 10^{16}\,\mathrm{cm}^{-3}$ and $T = 1\,\mathrm{eV}$ including, say, all discrete levels up to $n = \infty$. Submissions of all such results should include an adequate description of the model used in the `<comments>` field of the file (see Sec. 4).

2 Justification of cases and details

2.1 Reference cases

These cases are not necessarily realistic, but good for basic comparison and understanding what is wrong/different if there is a significant scatter in the results of more advanced cases below. There are quite a few sub-cases, however the models are simplest: ideal plasma (straight path trajectories and infinite Debye length for MD, or Holtsmark distribution for analytical approaches) and pure linear Stark effect (interactions between states with $\Delta n \neq 0$ ignored and no fine structure). In order to assess influence of electrons and ions (protons), we ask to calculate the broadening assuming e and p acting separately and together, i.e., three variants in total for each pair of n_e and T.

1. Hydrogen Lyman-α in an ideal plasma is a classical ion-dynamics test.
2. A relatively high-n line. For the plasma parameters selected, this is a test of the transition for electrons from dynamic to almost static regime.

Please note that all cases below do NOT assume an ideal plasma, unless explicitly said so.

2.2 High-n $\Delta n = 1$ transitions

A representative of $n, n' \gg 1, \Delta n \ll n$ class of transitions. Radio-frequency lines which are of great interest for astrophysics belong to it. We do not want to go to really high n, however, due to the computational costs. Nevertheless, we shall deal with the coupling between states with $\Delta n \neq 0$.

3. Hydrogen $n = 6 \to n = 5$ transition. We ask to calculate this case using three atomic models: (i) no $\Delta n \neq 0$ coupling accounted for, (ii) $n = 5$ and $n = 6$ states couple, and (iii) $n = 5$, 6, and 7 states included in the Hamiltonian and allowed to mix.

2.3 Isolated lines

First, the (in)famous Li-like 3s-3p sequence, with the divergence between QM calculations and experiments growing with Z [1]. Each of the three species (below) is asked to be calculated for a single representative density

Table 1: Case definitions.

ID	Transition(s)	# of subcases	n_e (cm^{-3})	T (eV)	Extra parameters
1	H Lyman-α	$3 \times 3 \times 3 \times 1 = 27$	10^{17}, 10^{18}, 10^{19}	1, 10, 100	—
			Model: $\Delta n \neq 0$ interactions ignored (strictly linear Stark effect); no fine structure; ideal plasma (straight path trajectories and infinite Debye length for MD or Holtsmark distribution for analytical models) in **three** variants: only electrons, only protons, and electrons and protons together.		
2	H Lyman-δ	$3 \times 3 \times 3 \times 1 = 27$	10^{16}, 10^{17}, 10^{18}	1, 10, 100	—
			Model: Same as above.		
3	H $n = 6 \rightarrow 5$	$2 \times 2 \times 3 \times 1 = 12$	5×10^{15}, 2×10^{16}	1, 10	—
			Model: $\Delta n \neq 0$ interactions included in **three** approximations: none, only $n = 5$ and 6 levels interact, and all from $n = 5$ to $n = 7$. Plasma ions: protons.		
4	Be II 3s-3p	$1 \times 3 \times 2 \times 1 = 6$	10^{17}	5, 15, 50	—
			Model: 3s, 3p, and 3d levels included, no fine structure. Only electron broadening included, in **two** approximations: straight paths and hyperbolic trajectories.		
5	N V 3s-3p	$1 \times 3 \times 2 \times 1 = 6$	10^{18}	5, 15, 50	—
			Model: Same as above.		
6	Ne VIII 3s-3p	$1 \times 3 \times 2 \times 1 = 6$	10^{19}	5, 15, 50	—
			Model: Same as above.		
7	Al III 4s-4p	$1 \times 3 \times 2 \times 1 = 6$	10^{18}	2, 4, 8	—
			Model: 4s, 4p, and 4d levels included, no fine structure. Plasma perturbations in **two** approximations: only electrons and both electrons and ions (Al III).		
8	Si XIII $n = 3 \rightarrow 1$	$3 \times 1 \times 1 \times 1 = 3$	10^{21}, 10^{22}, 10^{23}	300	—
			Model: $n = 1$ and 3 singlet levels only, ignoring $\Delta n \neq 0$ interactions. Plasma ions are protons.		
9	Al XIII Lyman-α	$2 \times 1 \times 2 \times 3 = 12$	10^{21},10^{22}	500	$\omega = 10^{15}$ rad/s, $F = 0, 1, 2$ GV/cm
			Model: $n = 1$ and 2 levels in **two** variants: with and without fine structure. Plasma ions are Al XIII, no electrons.		
10	D Balmer-α	$2 \times 2 \times 2 \times 3 = 24$	2×10^{14}, 10^{15}	1, 5	$B = 0, 5, 10$ T
			Model: with/without fine structure for the lower/higher density, respectively; ideal plasma in **two** variants: ions are either deutrons or infinitely massive particles.		
11	D Balmer-β	$2 \times 2 \times 2 \times 3 = 24$	2×10^{14}, 10^{15}	1, 5	$B = 0, 5, 10$ T
			Model: Same as above.		
12	D $n = * \rightarrow 2$	$3 \times 1 \times 2 \times 1 = 6$	10^{15}, 10^{16}, 10^{17}	1	—
			Model: fully ionized D plasma, LTE, **two** variants: only bound-bound transitions included or both bound-bound and free-bound.		
13	H Balmer-α	$1 \times 1 \times 2 \times 1 = 2$	10^{18}	1	—
			Model: linear Stark, plasma in **two** variants: ideal and interacting. Plasma ions: protons.		
14	H Balmer-β	$1 \times 1 \times 2 \times 1 = 2$	10^{18}	1	—
			Model: Same as above.		
15a	Ar XVII He-β	$3 \times 1 \times 1 \times 1 = 3$	5×10^{23}, 10^{24}, 2×10^{24}	1000	—
			Model: plasma ions are deutrons with 0.1% of Ar XVII.		
15b	Ar XVI He-β^* $n = 2$	$3 \times 1 \times 2 \times 1 = 6$	5×10^{23}, 10^{24}, 2×10^{24}	1000	—
15c	Ar XVI He-β^* $n = 3$	$3 \times 1 \times 2 \times 1 = 6$	5×10^{23}, 10^{24}, 2×10^{24}	1000	—
15d	Ar XVI He-β^* $n = 4$	$3 \times 1 \times 2 \times 1 = 6$	5×10^{23}, 10^{24}, 2×10^{24}	1000	—
			Atomic model: with and without the interference term in the electron broadening; plasma model: as above.		

and three values of the temperature. Only widths (FWHM) are requested. The plasma model for these cases consists only of electrons, and we ask to assume either straight path trajectories or more realistic quasi-classical hyperbolic trajectories (due to the Coulomb interaction with the radiator).

4. Be II is the first non-neutral species of the sequence.

5. N V — something in between.

6. Ne VIII is about the highest Z for which the 3s-3p broadening can be reliably measured.

In connection with the three previous cases, we consider another isolated line for which quantum effects are not expected to be so significant (larger matrix elements and cross-sections), i.e., a higher-n line.

7. Al III 4s-4p. In addition to the width, we also want to compare shifts, therefore, calculations with only electrons and e+ions are requested.

2.4 Intermediate case between isolated and degenerate regimes

8. He-like Si XIII $3 \rightarrow 1$ transitions. No inter-combination lines, only singlet levels. At the low density, only 1s-3p (He-β proper) is seen, then 1s-3d and 1s-3s appear as well, approaching Lyman-β-like shape at the highest density. Plasma ions are protons.

2.5 External fields

The external macro fields (both electric and magnetic) are always assumed to be parallel to the z axis.

9. Al XIII Lyman-α under external harmonic perturbation, e.g., a laser. The functional dependence of the electric field is $F\cos(\omega t)$, with ω and F given in Table 1. The two plasma densities correspond to laser-dominated and plasma-dominated line shapes. Two variants of the atomic model: with and without fine structure taken into account.

10. D Balmer-α in the presence of magnetic field, parameters typical for tokamaks. We want to investigate the difference between dynamic and (quasi)static ions (for MD codes, set the ion and radiator masses as large as possible).

11. Same for D Balmer-β.

2.6 High-n merging with continuum

These cases are rather advanced. It is interesting to see what different approaches use when several discrete levels start to overlap between themselves and continuum states. A broad spectral region will be analyzed covering both discrete and continuum spectrum and a transition region in between.

12. D Balmer series at $T = 1\,\mathrm{eV}$ and three densities, the lowest one about corresponding to tokamak conditions [2] (but no magnetic field in this case). The higher densities are typical for white dwarf photospheres [3].

2.7 Influence of particle correlations on electric micro-fields

In this set of cases the focus will be on analyzing the correlation properties of plasma fields on line shapes [4, 5]. To this end, a set of statistical properties of the micro-fields will be compared in each calculation case. These are (i) distributions of magnitudes of the "slow" and "fast" components of the total micro-field $\vec{F}(t) = \vec{F}_\mathrm{e}(t) + \vec{F}_\mathrm{i}(t)$, defined as

$$\vec{F}_\mathrm{slow}(\Delta t; t) = \int_{-\Delta t/2}^{\Delta t/2} \vec{F}(t - t')\mathrm{d}t' \tag{1}$$

and

$$\vec{F}_\mathrm{fast}(\Delta t; t) = \vec{F}(t) - \vec{F}_\mathrm{slow}(\Delta t; t)\,, \tag{2}$$

respectively, and (ii) correlations between directionalities of micro-field components

$$C_{ab}(\tau) = \int \mathrm{d}t \vec{\phi}_a(t) \cdot \vec{\phi}_b(t+\tau), \tag{3}$$

where

$$\vec{\phi}_a(t) = \frac{\vec{F}_a(t)}{F_a(t)}\,, \tag{4}$$

and the indices a and b represent either electrons (e) or ions (i).

13. H Balmer-α in two plasma model variants: without interactions between the plasma particles (ideal plasma) and with such interactions.

14. H Balmer-β. Same as above.

2.8 Satellite broadening

Another advanced case, satellites from the previous charge state with a spectator electron.

15. Ar XVII He-β and its Li-like satellites. The argon He-β composite spectral feature is observed in inertial confinement fusion implosion core plasmas when a tracer amount of argon is added to the deuterium gas fill to diagnose the plasma conditions. This spectral feature is comprised of the $n = 1$ to $n = 3$ line transition in He-like Ar and satellite line transitions in Li-like Ar. It is temperature and density sensitive through the density dependence of the Stark-broadened line shapes and the temperature and density dependence of the atomic level populations. In implosion core dense plasmas the Stark broadening effect dominates the line shapes. The details of these line shapes and their overlapping, impact the photon-energy dependent emissivity and opacity that, in turn, determine the emergent intensity distribution of the spectral feature and its diagnostic properties [6].

    Case 15a corresponds to Ar XVII He-β proper, and 15b,c,d to its Ar XVI $n = 2$, $n = 3$, and $n = 4$ spectator satellites, respectively.

    - Ar XVII He-β. Upper configurations: $1s3s$, $1s3p$, and $1s3d$; lower configurations: $1s^2$.
    - Ar XVI satellite transitions with spectator electron in $n = 2$. Upper configurations: $1s2s3s$, $1s2s3p$, $1s2s3d$, $1s2p3s$, $1s2p3p$, and $1s2p3d$; lower configurations: $1s^22s$, and $1s^22p$.
    - Ar XVI satellite transitions with spectator electron in $n = 3$. Upper configurations: $1s3s^2$, $1s3s3p$, $1s3s3d$, $1s3p^2$, $1s3p3d$, and $1s3d^2$; lower configurations: $1s^23s$, $1s^23p$, and $1s^23d$.
    - Ar XVI satellite transitions with spectator electron in $n = 4$. Upper configurations: $1s3s4s$, $1s3p4s$, $1s3d4s$, $1s3s4p$, $1s3p4p$, $1s3d4p$, $1s3s4d$, $1s3p4d$, $1s3d4d$, $1s3s4f$, $1s3p4f$, and $1s3d4f$; lower configurations: $1s^24s$, $1s^24p$, $1s^24d$ and $1s^24f$.

    Assume an equilibrium (i.e., LTE) distribution of population within the initial (upper) energy levels of the transitions within a given line shape.

3 Atomic data

In all cases, we assume the dipole approximation both for the radiation ($E1$) and the perturbation due to the plasma micro-fields. The relevant matrix elements are

$$\langle \alpha j m | r_q | \alpha' j' m' \rangle = (-1)^{j-m} \begin{pmatrix} j & 1 & j' \\ -m & q & m' \end{pmatrix} (\alpha j | r | \alpha' j')\,. \tag{5}$$

The reduced radius-vector matrix elements $(\alpha j|r|\alpha' j')$, relevant for the cases considered, are given below.

Table 2: Hydrogen reduced matrix elements up to $n = 5$.

	1s	2s	2p	3s	3p	3d	4s	4p	4d	4f	5s	5p	5d	5f
2p	-1.29	5.20												
3s			0.938											
3p	-0.517	-3.06		12.7										
3d			-6.71		14.2									
4s			0.382		2.44									
4p	-0.305	-1.28		-5.47		1.84	23.2							
4d			-2.418		-10.7			29.4						
4f						-17.7			27.5					
5s			0.228		0.970			4.60						
5p	-0.209	-0.774		-2.26		0.683	-8.52		4.31		36.7			
5d			-1.38		-4.20			-15.6		2.88		48.6		
5f						-5.75			-24.4				52.0	
5g										-35.4				45.0

3.1 Hydrogen-like

For hydrogen ($Z = 1$) and hydrogen-like cases, the data are to be calculated analytically. For cases where the fine structure is neglected, the binding energies to be assumed are (in atomic units $E_{\rm H} \approx 27.211\,{\rm eV}$, corresponding to $\approx 2.1947 \times 10^5\,{\rm cm}^{-1}$)

$$E_n^0 = -\frac{Z^2}{2n^2}\,. \tag{6}$$

When the fine structure is asked to be accounted for, the energies are

$$E_{nj} = E_n^0 - \frac{\alpha^2 Z^4}{2n^3}\left(\frac{1}{j+1/2} - \frac{3}{4n}\right)\,, \tag{7}$$

where $\alpha \approx 7.2974 \times 10^{-3}$ is the fine-structure constant.

Reduced matrix elements of radius-vector are

$$(n\ell|r|n'\ell') = Z^{-1}(-1)^{\ell+\ell_>}\sqrt{\ell_>}R_{n\ell}^{n'\ell'}\,, \tag{8}$$

where $\ell_> = \max(\ell, \ell')$ and

$$R_{n\ell}^{n\ell-1} = \frac{3}{2}n\sqrt{n^2-\ell^2} \tag{9}$$

for diagonal terms (e.g., Eq. (63.5) in [7]) and

$$R_{n\ell}^{n'\ell-1} = \frac{(-1)^{n'-\ell}}{4(2\ell-1)!}\sqrt{\frac{(n+\ell)!(n'+\ell-1)!}{(n-\ell-1)!(n'-\ell)!}}\frac{(4nn')^{\ell+1}(n-n')^{n+n'-2\ell-2}}{(n+n')^{n+n'}}\times$$
$$\left\{F_{21}\left(-n_r, -n_r', 2\ell, -\frac{4nn'}{(n-n')^2}\right) - \left(\frac{n-n'}{n+n'}\right)^2 F_{21}\left(-n_r-2, -n_r', 2\ell, -\frac{4nn'}{(n-n')^2}\right)\right\} \tag{10}$$

for off-diagonal ones (Eq. (63.2) in [7]). Here, F_{21} is the Gauss hypergeometric function and $n_r = n - \ell - 1$, $n_r' = n' - \ell$ are the radial quantum numbers of the two states. For convenience, the reduced matrix elements up to $n = 5$ are given in Table 2.

3.2 Non-hydrogen

The data are taken from the NIST on-line compilation [8][1]. The level energies, averaged over the fine-structure components for $\ell > 0$, are given in Table 3. The absolute values of the matrix elements are obtained from the respective multiplet-averaged absorption oscillator strengths f according to

$$|(n\ell|r|n'\ell')| = \sqrt{\frac{3f(2\ell'+1)}{2(E_{n\ell} - E_{n'\ell'})}}\,, \tag{11}$$

[1] Except for the Ne VIII 3p–3d oscillator strength, in which a typo is apparently made. For this transition, we use [9] instead.

Table 3: Atomic level energies.

Species	Level	Energy (cm^{-1})
Be II	3s	88231.915
	3p	96496.645
	3d	98054.888
N V	3s	456126.60
	3p	477816.57
	3d	484417.50
Ne VIII	3s	1099870.00
	3p	1135149.33
	3d	1147450.00
Al III	4s	126164.05
	4p	143686.79
	4d	165786.80
Si XIII	$1s^2\ ^1S$	0.0
	$1s3s\ ^1S$	17579166.0
	$1s3p\ ^1P$	17603422.0
	$1s3d\ ^1D$	17599605.0

Table 4: Matrix elements.

Species	Transition	f	$(\|r\|)$
Be II	3s — 3p	8.298e-01	5.75
	3p — 3d	8.108e-02	7.17
N V	3s — 3p	3.95e-01	2.45
	3p — 3d	5.48e-02	2.86
Ne VIII	3s — 3p	2.51e-01	1.53
	3p — 3d	3.82e-02	1.75
Al III	4s — 4p	1.29e+00	4.92
	4p — 4d	1.30e+00	7.62

and sign as in respective H-like from Eqs. (8 – 10). The data are summarized in Table 4. For Si XIII, hydrogen-like matrix elements ($Z = 13$) between the $n = 3$ states should be used, which are accurate to within $\sim 1\%$.

3.3 Data for cases 15*

Atomic physics files computed with R. Cowan's atomic structure code [10] are provided for the four line shape calculations, namely the argon He-β line transition, and the Li-like Ar transitions with spectator electron in $n = 2$, $n = 3$ and $n = 4$. Each atomic physics data file contains the list of fine structure energy levels for the set of upper and lower configurations including energy value, parity and total angular momentum J, and reduced electric-dipole matrix elements between the levels.

Due to the vast amount of data for these cases, they are provided as attachments, formatted as follows:

1. First record: only the first four numbers are relevant, namely
   $Z \quad \chi \quad NJI \quad NJF$,
   where Z: atomic number, χ: net ion charge, NJI: number of initial (upper) energy levels, NJF: number of final (lower) energy levels.

2. Second record: the numbers on this record are not relevant.

3. Following up the second record, there are NJT = NJI + NJF records with the information of the energy levels. First, NJI records for the initial energy levels, then NJF records for the final energy levels. One record per energy level with the following structure,
   $L \quad J \quad E$ Alpha,

where L: the integer label of the energy level, J: total angular momentum of the level, E: energy of the level in $1000\,\mathrm{cm}^{-1}$ (to convert to eV multiply by 0.12398), Alpha: an alphanumeric string showing the leading configuration in the level (i.e. parity).

4. Following up the NJT records with the energy level structure information, there are a number of records with the information of the line transitions. One record per line transition with the following structure,
$L1$ $L2$ Rdme ΔEa ΔEb λ Type,
where $L1$, $L2$: integer labels of the levels of the line transition, Rdme: reduce dipole matrix element in atomic units, ΔEa: energy of the transition in $1000\,\mathrm{cm}^{-1}$, ΔEb: energy of the transition in eV, λ: wavelength of the transition in Å, Type: index of type of transition, 1 for electric dipole. Only electric dipole transitions are included in the file.

Ar XVII: he_beta.txt

Ar XVI $n = 2$ satellites: he_beta_sat2.txt

Ar XVI $n = 3$ satellites: he_beta_sat3.txt

Ar XVI $n = 4$ satellites: he_beta_sat4.txt

(Click on the *.txt links above to download the data attached. If your PDF viewer is unable to display the attachments, you can download all data files in a single archive, http://plasma-gate.weizmann.ac.il/uploads/slsp/he_beta_data.zip.)

4 Submission format

We use an XML-based format for submissions, with an example shown schematically in Listing 1.

Everything is included between the <slsp> and </slsp> tags. The meaning of other tags is described below:

<case> The subcase identification in the Case_ID.N.T.M.F format, see Sec. 1.

<contributor> The person who submits these results.

<affiliation> His/her affiliation.

<code> Name of the code/approach.

<version> Version of the code (optional).

<date> Date/time when the calculations were made.

<comments> Any comments you may like to make. The comments are optional, **except for advanced models (M=0 in the subcase id)**. In the later cases, please describe the model employed with sufficient details. If the comments must contain "<" or "&" characters, enclose the entire text with "<![CDATA[" and "]]>":

```
<comments><![CDATA[
  Some bizarre & < > comments.
]]></comments>
```

<time1> Physical time (not CPU!), in seconds, the evolution of the atomic system is calculated for in a single run. (This and the following entry are specific for MD simulations. When irrelevant, skip or set to zero.)

<nruns> Number of runs used for averaging.

<accuracy> The estimated accuracy (in %) of the calculations, say of the FWHM. Only uncertainties introduced by the calculations should be included (in particular, not those due to an idealized/simplified plasma or atomic models suggested for this specific case). If the error bars are asymmetric, list two numbers with proper signs.

Listing 1: An example of submission.

```
<?xml version="1.0"?>
<slsp>
  <case>1.1.1.3.1</case>
  <contributor>E. Stambulchik</contributor>
  <affiliation>WIS</affiliation>
  <code>simu</code>
  <version>1.9.0/1.4.0</version>
  <date>2011-12-13 18:34:39</date>

  <comments>
     These are my comments on this calculation.
  </comments>

  <time1>6.826e-11</time1>
  <nruns>400</nruns>

  <accuracy>-10 +5</accuracy>

  <field_distribution unit="128196">
    0.000000 0.000000
    0.025000 0.000421
    0.075000 0.002919
      ...
      ...
    29.875000 0.000333
    29.925000 0.000324
    29.975000 0.000316
  </field_distribution>

  <spectrum unit="1">
    -200.0 0.000741852
    -199.8 0.000751194
    -199.6 0.000747932
      ...
      ...
    199.6 0.000738701
    199.8 0.000752916
    200.0 0.000735306
  </spectrum>
</slsp>
```

`<spectrum>` For all cases **except those concerned with isolated lines (4 – 7)**, we ask to provide entire line shapes on a reasonably dense grid, typically $\sim$ 1000 points (see Table 5). When the spectral range is symmetric ($\pm$ something), it means relative to the unperturbed position ω_0, calculated as a difference between the weighted-average energies of the initial and final levels:

$$\hbar\omega_0 = \frac{\sum_i g_i E_i}{\sum_i g_i} - \frac{\sum_f g_f E_f}{\sum_f g_f} \,. \tag{12}$$

The spectral windows and distances between the consecutive abscissas defined are recommended values. The relatively wide spectral windows are defined on purpose, to investigate far wings of the spectral lines. You can use denser and/or wider grids as you see fit. It is suggested to use equidistant grids. The units are cm^{-1}. The optional `unit` attribute allows for scaling the abscissas, e.g., by using `unit="8065.5"` one can output spectra in eV's. Where the spectra are requested and external fields specified (cases 9, 10, and 11), the π ($\Delta M = 0$) and σ ($\Delta M = \pm 1$) polarizations will be needed separately (to be provided as the second and third columns, respectively):

```
...
...
<spectrum>
  w_1 I_pi(w_1) I_sigma(w_1)
  w_2 I_pi(w_2) I_sigma(w_2)
  ...
  ...
  w_N I_pi(w_N) I_sigma(w_N)
</spectrum>
...
...
```

It is assumed that

$$I_{\mathrm{tot}}(\omega) = I_\pi(\omega) + 2I_\sigma(\omega) \,. \tag{13}$$

No normalization condition is imposed (you can use peak- or area-normalized profiles).

`<field_distribution>` Quasi-static field distribution (normalized) used for the calculation (due to all plasma particles, but excluding external fields, if any). The fields are in V/cm. The optional `unit` attribute allows for scaling the field strength values conveniently, e.g., by setting it to the Holtsmark normal field strength F_0 one obtains the distribution of the reduced field strengths. The distributions should be calculated on an equidistant grid covering at least $0 - 10$ with a step not exceeding 0.1 (in units of F_0). **In addition, for cases 13 and 14,** distributions of magnitudes of the "slow" and "fast" microfield components, defined by Eqs. (1) and (2), are requested. The distributions should be calculated for $\Delta t = \{0.1, 0.3, 1, 3, 10\} \times 10^{-14}\,\mathrm{s}$. These are to be presented like in the listing below:

```
...
...
<field_distribution delta_t="1e-15">
  F_1 W_slow(F_1) W_fast(F_1)
  F_2 W_slow(F_2) W_fast(F_2)
  ...
  ...
  F_N W_slow(F_N) W_fast(F_N)
</field_distribution>

<field_distribution delta_t="3e-15">
  ...
  ...
</field_distribution>
...
...
```

`<width>` FWHM, **for isolated lines only (cases 4 – 7)**. In units of cm^{-1}.

Table 5: Spectral grids.

Subcase	Spectral range (cm^{-1})	Step (cm^{-1})
1.1.*.*.*	$\pm$ 200	0.2
1.2.*.*.*	$\pm$ 1,000	1
1.3.*.*.*	$\pm$ 5,000	5
2.1.*.*.*	$\pm$ 1,000	3
2.2.*.*.*	$\pm$ 5,000	20
2.3.*.*.*	$\pm$ 25,000	100
3.1.*.*.*	$\pm$ 200	1
3.2.*.*.*	$\pm$ 400	2
8.1.*.*.*	$\pm 5 \times 10^4$	100
8.2.*.*.*	$\pm 10^5$	500
8.3.*.*.*	$\pm 5 \times 10^5$	1000
9.*.*.*.*	$\pm 5 \times 10^4$	50
10.1.*.*.*	$\pm$ 20	0.04
10.2.*.*.*	$\pm$ 50	0.1
11.1.*.*.*	$\pm$ 100	0.2
11.2.*.*.*	$\pm$ 250	0.5
12.1.*.*.*	$(2.4 - 3.0) \times 10^4$	3
12.2.*.*.*	$(2.0 - 3.0) \times 10^4$	5
12.3.*.*.*	$(2.0 - 3.0) \times 10^4$	20
13.*.*.*.*	$\pm$ 1,000	3
14.*.*.*.*	$\pm$ 5,000	15
15.*.*.*.*	$\pm 2 \times 10^6$	4000

`<shift>` Shift, **only for case 7**. In units of cm^{-1}.

`<field_correlation>` **For cases 13 and 14 only.** Correlations between directionalities of micro-field components, see Eq. (3). We ask for all three C_{ee}, C_{ii}, and C_{ei} over τ from 10^{-16} s to 10^{-11} s on a *logarithmic* grid of 100 points at least:

```
...
...
<field_correlation>
  tau_1 C_ee(tau_1) C_ii(tau_1) C_ei(tau_1)
  tau_2 C_ee(tau_2) C_ii(tau_2) C_ei(tau_2)
  ...
  ...
  tau_N C_ee(tau_N) C_ii(tau_N) C_ei(tau_N)
</field_correlation>
...
...
```

References

[1] Yu. V. Ralchenko, H. R. Griem, and I. Bray. Electron-impact broadening of the 3s-3p lines in low-Z Li-like ions. *J. Quant. Spectr. Rad. Transfer*, 81:371–384, 2003.

[2] A. Yu. Pigarov, J. L. Terry, and B. Lipschultz. Study of the discrete-to-continuum transition in a Balmer spectrum from Alcator C-Mod divertor plasmas. *Plasma Phys. Control. Fusion*, 40:2055–2072, 1998.

[3] P.-E. Tremblay and P. Bergeron. Spectroscopic analysis of DA white dwarfs: Stark broadening of hydrogen lines including nonideal effects. *Astrophys. J.*, 696(2):1755–1770, May 2009.

[4] E. Stambulchik, D. V. Fisher, Y. Maron, H. R. Griem, and S. Alexiou. Correlation effects and their influence on line broadening in plasmas: Application to H_α. *High Energy Density Phys.*, 3:272–277, 2007.

[5] A. Calisti, B. Talin, S. Ferri, C. Mossé, V. Lisitsa, L. Bureyeva, M. A. Gigosos, M. Á. González, T. del Río Gaztelurrutia, and J. W. Dufty. Electric micro fields in simulated two component plasmas. In M. A. Gigosos and M. Á. González, editors, *SPECTRAL LINE SHAPES: Volume 15 19th International Conference on Spectral Line Shapes*, volume 1058, pages 27–33, Valladolid (Spain), 2008. AIP.

[6] I.E. Golovkin and R.C. Mancini. High-order satellites and plasma gradients effects on the Ar He_β line opacity and intensity distribution. *J. Quant. Spectr. Rad. Transfer*, 65(1–3):273–286, 2000.

[7] Hans A. Bethe and Edwin E. Salpeter. *Quantum Mechanics of One- and Two-Electron Atoms*. Plenum, New York, 1977.

[8] NIST atomic spectra database. http://www.nist.gov/pml/data/asd.cfm.

[9] W. L. Wiese, M. W. Smith, and B. M. Glennon. *Atomic transition probabilities. Vol. I: Hydrogen through Neon. A critical data compilation*. US Department of Commerce, National Buereau of Standards, Washington, D.C., 1966.

[10] R.D. Cowan. *The Theory of Atomic Structure and Spectra*. University of California Press, Berkeley - Los Angeles - London, 1981.